ELSEVIER

Journal of Organometallic Chemistry 579 (1999) 114–121

Journal of Organometallic Chemistry

Probing diruthenium σ-alkynyl bonding interactions via substituent effects. Linear free energy relationships in dinuclear compounds VI☆

Chun Lin [a], Tong Ren [a,b,*], Edward J. Valente [c], Jeffrey D. Zubkowski [d]

[a] *Department of Chemistry, Florida Institute of Technology, Melbourne, FL 32901, USA*
[b] *Department of Chemistry, University of Miami, Coral Gables, FL 33124, USA*
[c] *Department of Chemistry, Mississippi College, Clinton, MS 39058, USA*
[d] *Department of Chemistry, Jackson State University, Jackson, MS 39217, USA*

Received 30 June 1998; received in revised form 16 November 1998

Abstract

Several paramagnetic tetrakis(diarylformamidinato)diruthenium(II,III) complexes bearing one phenylethynyl ligand at the axial position, $Ru_2(ArNC(H)NAr)_4(C{\equiv}CPh)$ (Ar as *p*-ClC_6H_4 (**2**), *m*-ClC_6H_4 (**3**), *m*-$CF_3C_6H_4$ (**4**), 3,4-$Cl_2C_6H_3$ (**5**), and 3,5-$Cl_2C_6H_3$ (**6**)), were prepared and characterized. Cyclic voltammetry studies of **2**–**6** revealed the presence of two one-electron redox couples: Ru_2^{6+}/Ru_2^{5+} and Ru_2^{5+}/Ru_2^{4+}, and the half-wave potential for the latter correlates linearly with the Hammett constant (σ) of the aryl substituent. Molecular structures of **3** and **6** were determined by X-ray crystallography. The nature of $Ru_2{-}C{\equiv}C$ bonding interaction was predominantly $Ru{-}C_\alpha$ σ-bonding based on the substituent-dependence of $\upsilon(C{\equiv}C)$, which decreases linearly with the increase of the Hammett constant σ of substituent.

Keywords: Diruthenium complexes; Diarylformamidinates; Phenylethynyl; Hammett correlation

1. Introduction

The past 15 years have witnessed a phenomenal growth in the body of knowledge about compounds containing metal–alkynyl σ-bonds, as indicated by a recent comprehensive review [2] and a monograph [3]. Among many investigative efforts gearing towards material applications, early attempts to construct *molecular wires* based on main-chain polymetallaynes of group 10 metals by the laboratories of Takahashi and Hagihara [4] and Lewis [5] are noteworthy. More recently, large quadratic and cubic optical nonlinearities have been achieved with both ruthenium(II)- and gold(I)-σ-arylacetylide complexes by Humphrey [6]. Terminal Pd/Pt-alkynyl species with a square-planar coordination geometry have been extensively used as the building units in the self-assembly of 'molecular squares' and other molecular polygons by Stang [7].

For the construction of molecular materials containing metal–alkynyl σ-bonds, control and optimization of $M{-}C{\equiv}C$ π interactions are often the focus, since these interactions are key to achieving efficient electronic couplings among the molecular building units, which in turn determines the properties of materials [3,8]. Therefore, much of the recent literature has emphasized the experimental quantification of $M{-}C{\equiv}C$ π interactions through the comparison of both structural and IR spectroscopic data for the C≡C bond [2].

Metal–metal bonded dinuclear complexes containing σ-bonded alkynyl ligands are less common than mononuclear complexes containing σ-bonded alkynyl groups. The dinuclear complexes can be categorized into two structural classes: the ones with the axially coordinated alkynyl ligands (motif I in Scheme 1), and

☆ For Part V, see Ref. [1].

* Corresponding author. Tel.: +1-305-284-6617; fax: +1-305-284-1880.

E-mail address: tren@umiamil.ir.miami.edu (T. Ren)

0022-328X/99/$ - see front matter
PII: S0022-328X(98)01211-X

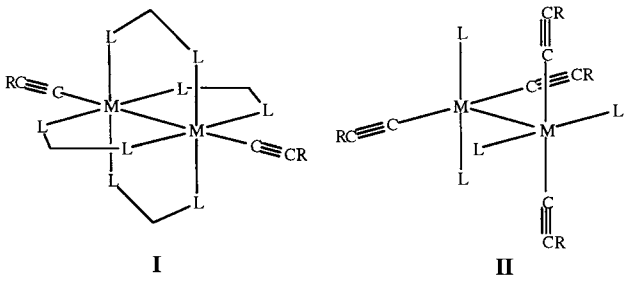

Scheme 1.

those with the equatorially coordinated alkynyl ligands (motif II in Scheme 1). The first of this type of compounds was $Ru_2(ap)_4(C{\equiv}CPh)$ reported by Cotton [9], where ap is 2-anilinopyridinate and the phenylethynyl ligand is axially coordinated to the Ru_2 core. Analogous mono- and di-alkynyl axial adducts of diruthenium and dirhodium cores have been studied by Bear et al. [10–13]. Compounds of structural motif II based on group 6 metals (Mo and W) were prepared and extensively characterized by Hopkins et al. [14]. Previously, we reported the synthesis and characterization of a diamagnetic series $Ru_2(form)_4(C{\equiv}CC_6H_5)_2$ (motif I) with the bridging ligand *form* as diarylformamidinate [1]. Herein, we wish to report the study of the monoadduct tetrakis(μ-*N*,*N*′-diarylformamidinato)-(η^1-phenylethynyl)diruthenium(III,II) family (Ru_2-$(form)_4(C{\equiv}CC_6H_5)$, Scheme 2), where a systematic attenuation of $\upsilon(C{\equiv}C)$ upon the change of electron-richness of the Ru_2 core has been observed.

2. Results and discussion

2.1. Synthesis of $Ru_2(form)_4(C{\equiv}CPh)$

Compounds **2**–**6** (Scheme 2) were prepared by the procedure similar to that reported for **1** (X as H) [12]. Treating the parent compound $Ru_2(form)_4Cl$ [15] with lithiated phenyl acetylene (50-fold excess) in THF affords the intermediate $[Ru_2(form)_4(CCPh)_2]^-$, which upon solvent removal in vacuo readily dissociates one of the axially bonded phenylethynyls to form the desired mono-adduct. In contrast to the reported instability of **1** to silica [12], compounds **2**–**6** were readily purified with silica column chromatography and the purities were confirmed by excellent elemental analysis. Both the increased stability and the significantly improved synthetic yield for **2**–**6** are likely to be attributed to the presence of the electron withdrawing phenyl substituent.

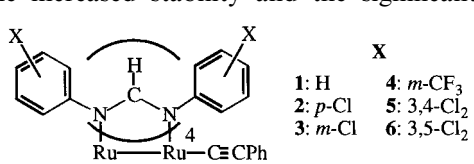

X

1: H **4**: *m*-CF_3
2: *p*-Cl **5**: 3,4-Cl_2
3: *m*-Cl **6**: 3,5-Cl_2

Scheme 2.

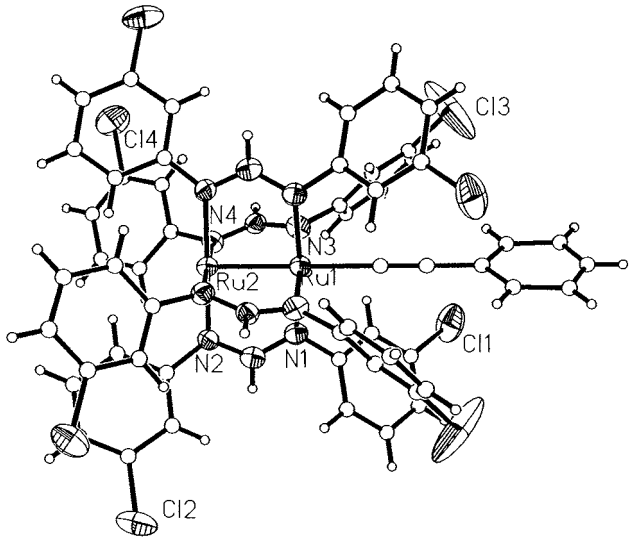

Fig. 1. The ORTEP plot of compound **3**.

2.2. Molecular structures of compounds **3** and **6**

The ORTEP diagrams of both compounds **3** and **6** are shown respectively in Figs. 1 and 2, and selected bond lengths and angles are listed in Table 1. Hexane-solvated compound **3** crystallized in the monoclinic space group $P2/n$. Compound **6** co-crystallized with four dichloromethane molecules in the orthorhombic space group *Pbcn*. Despite differences in space groups, molecules **3** and **6** and the previously published molecule **1** [12] all contain a crystallographic two fold axis passing through the $Ru-Ru-C-C$ vector, which relates one half of the molecule to the other half. The co-linear geometry of the Ru–Ru and C≡C bonds, as required by the crystallographic symmetry, is in

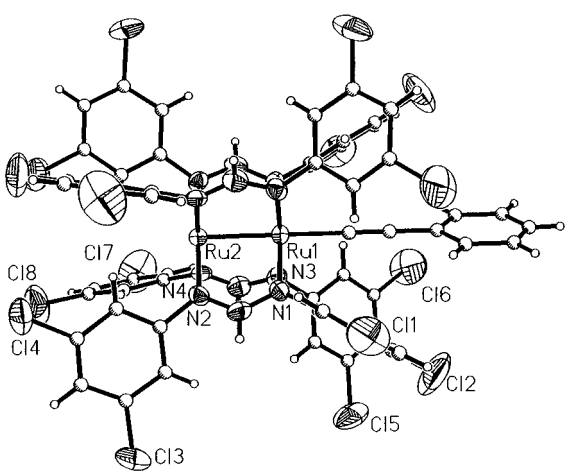

Fig. 2. The ORTEP plot of compound **6**.

Table 1
Selected bond distances (Å) and angles (°) for compounds **3** and **6**

Ru_2(*m*-Clform)$_4$(CCPh) (**3**)		Ru_2(3,5-Cl_2form)$_4$(CCPh) (**6**)	
Ru(1)–Ru(2)	2.3868(10)	Ru(1)–Ru(2)	2.4285(11)
Ru(1)–C(27)	2.057(9)	Ru(1)–C(51)	2.036(9)
C(27)–C(28)	1.191(11)	C(51)–C(52)	1.197(12)
Ru(1)–N(3)	2.110(4)	Ru(1)–N(1)	2.075(6)
Ru(1)–N(1)	2.117(4)	Ru(1)–N(3)	2.089(6)
Ru(2)–N(4)	2.051(4)	Ru(2)–N(4)	2.025(6)
Ru(2)–N(2)	2.049(4)	Ru(2)–N(2)	2.042(6)
N(1)–C(7)	1.304(6)	N(1)–C(1)	1.318(8)
N(2)–C(7)	1.333(6)	N(2)–C(1)	1.332(8)
N(3)–C(20)	1.305(6)	N(3)–C(2)	1.317(8)
N(4)–C(20)	1.321(6)	N(4)–C(2)	1.317(8)
C(27)–Ru(1)–Ru(2)	180.0	C(51)–Ru(1)–Ru(2)	180.0
C(28)–C(27)–Ru(1)	180.0	C(52)–C(51)–Ru(1)	180.0
N(3)–Ru(1)–Ru(2)	87.74(12)	N(1)–Ru(1)–Ru(2)	87.54(15)
N(1)–Ru(1)–Ru(2)	86.60(11)	N(3)–Ru(1)–Ru(2)	87.27(15)
N(4)–Ru(2)–Ru(1)	89.55(12)	N(4)–Ru(2)–Ru(1)	89.15(15)
N(2)–Ru(2)–Ru(1)	90.24(11)	N(2)–Ru(2)–Ru(1)	89.34(15)
C(7)–N(1)–Ru(1)	119.0(3)	C(1)–N(1)–Ru(1)	120.4(5)
C(7)–N(2)–Ru(2)	117.8(3)	C(1)–N(2)–Ru(2)	119.8(5)
C(20)–N(3)–Ru(1)	117.8(4)	C(2)–N(3)–Ru(1)	119.7(5)
C(20)–N(4)–Ru(2)	118.0(3)	C(2)–N(4)–Ru(2)	120.9(5)

stark contrast with the pronounced distortion observed in the bis-adducts, where the Ru–Ru–C_α angle is 159° and the deviation from the co-linearity was attributed to a second order Jahn–Teller effect [1].

The key geometric parameters around the diruthenium core of **3** and **6** are very similar, as shown by Table 1. At first glance, the Ru–Ru bond lengths in **3** (2.3868(10) Å) and **6** (2.4285(11) Å) appear to suggest a dependence of the Ru–Ru bond strength on the nature of the aryl substituents. However, the difference between the Ru–Ru bond lengths determined for the two independent molecules of **1** [12], 2.369(1) and 2.431(1) Å, is even larger, implying the sensitivity of Ru–Ru bond towards factors other than intramolecular bonding interactions. The difference in Ru–Ru bond lengths between **3** and **6** may thus be attributed to lattice packing effects. Of course these bond lengths are all within the expected range for Ru_2^{5+} paddlewheel species [16]. Reflecting the steric effect of axial phenylethynyl, the bridging-formamidinates exhibit an unsymmetric bidentate coordination mode: Ru(III) – N and Ru(II)–N bond lengths are 2.113 [4] and 2.052 [4] Å for **3**, and 2.082 [6] and 2.034 [6] Å for **6**.

In a comparison of the Ru–C and C≡C bond lengths among structurally known mono-alkynyl adducts: the former are, respectively 2.037(7)/2.018(7), 2.057(9), 2.036(9) Å for **1**, **3** and **6**, while the latter are 1.191(13)/1.216(12)/1.237(9), 1.196(11), and 1.197(12) Å. Since the variances are within the statistical range (3σ), the substituent-influence on the Ru_2–C≡C interaction cannot be discerned on the basis of X-ray structural data. This is consistent with previous studies of the isostructural series (PPh_3)Au(σ-arylethynyl) [17] and (η^5-Cp)(PPh_3)Ni(σ-arylethynyl) [18], where constant M–C_α and C_α≡C_β bond lengths were observed.

2.3. Electrochemistry

Half-wave electrode potentials for compounds **2**–**6** measured by cyclic voltammetry are tabulated in Table 2 and the cyclic voltammograms are shown in Fig. 3. Similar to the previously reported compound **1** [12], all of the compounds but **5** undergo two one-electron processes: oxidation (A) and reduction (B), as noted in Eqs. (1a), (1b):

$$Ru_2^{6+} + e^- \leftrightharpoons Ru_2^{5+} \text{ (reaction A)} \quad (1a)$$

$$Ru_2^{5+} + e^- \leftrightharpoons Ru_2^{4+} \text{ (reaction B)} \quad (1b)$$

The electrode potentials for reaction B, observed for compounds **2**–**6**, gradually shift anodically with an increase in the electron-withdrawing characteristics of the aryl substituents. The trend is consistent with the observation for series containing both Ru_2 and other transition metal cores [1,15,19–21]. Oxidation reaction A was observed as a quasi-reversible process for compounds **2**–**4**, and a irreversible process for **6**, and not observed for **5**. Such behavior implies that the Ru_2^{5+} core becomes more difficult to oxidize with an increase in the electron withdrawing ability of the aryl substituents.

Table 2
Experimental data for compounds **2**–**6**

X(σ)	*p*-Cl(0.23)	*m*-Cl(0.37)	*m*-CF_3(0.43)	3,4-Cl_2(0.60)	3,5-Cl_2(0.74)
$E_{1/2}$(A) (mV) [a]	641	724	814	NA	999 [b]
(ΔE_p, $i_{p,c}/i_{p,a}$)	(142, 0.80)	(179, 0.71)	(189, 0.35)	NA	NA
$E_{1/2}$(B) (mV) [a]	−537	−507	−408	−295	−226
(ΔE_p, $i_{p,c}/i_{p,a}$)	(101, 1.13)	(174, 1.01)	(106, 1.04)	(124, 1.08)	(107, 0.98)
ν(C≡C) (cm^{-1})	2045.0	2042.0	2041.0	2034.4	2030.6
λ_{max} (nm) (ε ($M^{-1}cm^{-1}$))	597(sh), 533 (8610), 381(sh)	590(sh), 526 (8530), 379(sh)	585(sh), 520 (9345), 373(sh)	588(sh), 536 (8945), 379(sh)	598(sh), 527 (8790), 379(sh)
μ_{eff} (BM)	3.61	3.92	3.60	3.79	3.99

[a] Measured with the scan rate of 100 mV s^{-1}.
[b] Irreversible, reported here is $E_{p,a}$ value.

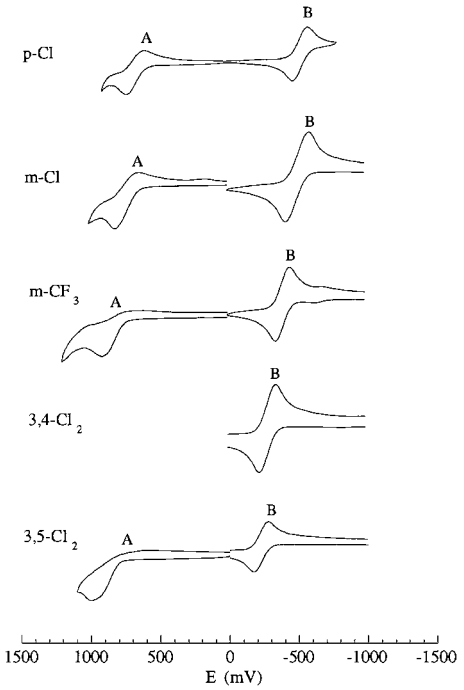

Fig. 3. Cyclic voltammograms of compounds **2**–**6** recorded in CH_2Cl_2 with the scan rate of 100 mV s^{-1}.

For reaction B, the dependence of $E_{1/2}(X)$ on the aryl substituent can be quantified using the Hammett correlation [20,22] according to:

$$E_{1/2}(X)/\text{mV} = \text{constant} + \rho(8\sigma) \quad (2)$$

Linear least-squares fit of electrode potentials of **2**–**6** yields a ρ (reactivity constant) of 82.1 mV with a correlation coefficient of 0.98. The fit also yields the constant in Eq. (2) as -710 mV, which should correspond to the electrode potential of the unsubstituted species **1**, i.e. $E_{1/2}(H)$, but cannot be directly compared with the previously reported datum for **1** (-890 mV vs. SCE, 0.1 M Bu_4NClO_4) [12] since different reference electrode and supporting electrolyte were used.

When comparing the $E_{1/2}(Ru_2^{5+}/Ru_2^{4+})$ values obtained for complexes $Ru_2(form)_4Cl$ [15], $Ru_2(form)_4(C{\equiv}CPh)$, and $Ru_2(form)_4(C{\equiv}CPh)_2$ [1] supported by the same formamidinate ligand, the electrode potential is shifted cathodically by about 200 mV upon the substitution of an axial chloro ligand with phenylethynyl, and further cathodically shifted by 700 mV with the addition of a second phenylethynyl. Obviously, the diruthenium(II,III) core is greatly stabilized with respect to reduction to the diruthenium(II,II) core by the coordination of the phenylethynyl ligand, a much stronger nucleophile than the chloro ligand. Similarly, the $E_{1/2}(Ru_2^{6+}/Ru_2^{5+})$ values for both compounds **2** and **3** are shifted cathodically by 130 mV from the corresponding $Ru_2(form)_4Cl$ compounds [15], reflecting a significant destabilization of the diruthenium(II,III) core with respect to oxidation to the diruthenium(III,III) core. The same trend has been observed in previous studies of **1** [12], and Ru_2(2-anilinopyridinate)$_4L_{ax}$ ($L_{ax} = Cl^-$ and $PhC{\equiv}C^-$) [9].

2.4. Electronic structures and electronic spectra

The room temperature (293 K) effective magnetic moments for compounds **2**–**6** range from 3.60 to 3.99 BM, clearly indicating the presence of three unpaired electrons. This observation is consistent with a ground state electronic configuration of $\sigma^2\pi^4\delta^2\delta^{*1}\pi^{*2}$, identical to that of the parent compounds $Ru_2(form)_4Cl$ [15] and also common to many Ru_2(II,III) paddlewheel complexes [16].

Table 2 summarizes the features of the electronic absorption spectra of **2**–**6** recorded in CH_2Cl_2 solutions (Fig. 4). A typical spectrum consists of one well-resolved peak around 530 nm and two shoulders around 590–380 nm. Due to the lack of proper MO calculations, a precise assignment of the observed bands is not available in the current study. Nevertheless, the similarity in absorption spectra among **2**–**6** clearly indicates a minimal substituent-perturbation of the distribution of upper valence molecular orbitals, as previously observed and elaborated for other dinuclear species [20,21].

2.5. IR spectroscopy and Ru_2–C≡C bonding

The C≡C-stretching frequencies (ν(C≡C)) for **2**–**6** obtained from FT-IR spectra are provided in Table 2. The frequencies, ranging from 2031 to 2045 cm^{-1}, are significantly lower than the ones observed for the bisphenylethynyl adducts $Ru_2(form)_4(C{\equiv}CPh)_2$ (2100 ± 2

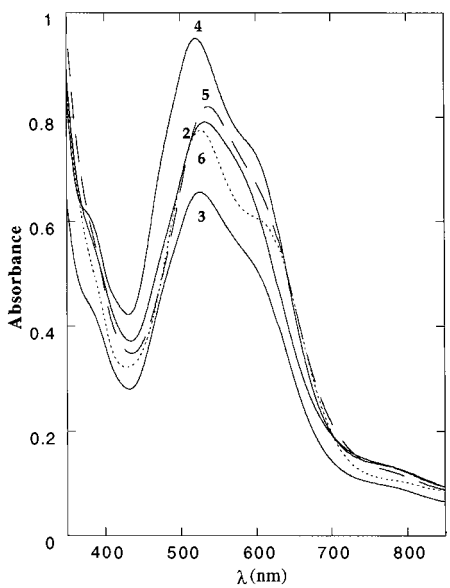

Fig. 4. UV-Vis spectra of compounds **2**–**6** recorded in CH_2Cl_2; **2** = 92 μM, **3** = 77 μM, **4** = 102 μM, **5** = 92 μM, and **6** = 88 μM.

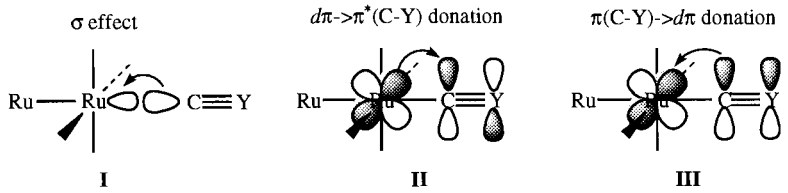

Scheme 3.

cm^{-1}) [1] and $Ru_2(F_5ap)_4(C{\equiv}CPh)_2$ (2093 cm^{-1}, where F_5ap is 2-(2,3,4,5,6-pentafluoroanilino)pyridinate) [13], but higher than that reported for $Mo_2(PR_3)_4(C{\equiv}CR)_4$ (1991 cm^{-1}) [14,23]. With an increase in the electron withdrawing ability of the aryl substituent of the formamidinate ligands, the ν(C≡C) value decreases, reflecting the resultant weakening of the C≡C bond. A linear correlation exists between the value of ν and the Hammett constant (σ):

$$\nu(C{\equiv}C) = a + \rho(8\sigma) \quad (3)$$

where the reactivity constant ρ is -3.68 cm^{-1}, and the correlation coefficient is 0.992. The constant a, 2053 cm^{-1}, should correspond to the ν(C≡C) value of **1**, the unsubstituted species, which was not reported [12].

As noted for both compounds **1**–**6** (Section 2.2) and transition metal–alkynyl complexes in general [2], X-ray structural data do not provide conclusive evidence about the nature of the M–C≡C interactions, especially with regard to the metal-to-alkynyl π-backdonation ($d\pi(M) \rightarrow \pi^*(C{\equiv}C)$). A more sensitive alternative in gauging the $d\pi \rightarrow \pi^*$ interaction is the ν(C≡C) value, provided that the complication of symmetry-allowed mixing with ν(C–R) is eliminated by the use of the same C≡CR group [2]. Notably, Bianchini et al. reported an increase of 45 cm^{-1} in ν(C≡C) upon varying the oxidation state of Rh from $+1$ to $+3$ for several structurally related Rh–alkynyl complexes [24], supporting a significant $d\pi(Rh) \rightarrow \pi^*$(acetylide) charge transfer in the Rh(I) complexes. By increasing the electron occupancy in the π-donor orbital δ*(MoMo) in $Mo_2(CCSiMe_3)_4(PMe_3)_4$ both electrochemically and photochemically, Hopkins et al. observed a decrease in the value of ν(C≡C) as large as 109 cm^{-1} [23], a truly remarkable change. The ν(C≡C) data obtained for **2**–**6**, although within a modest range, suits this purpose well since the only variable is the substituent on the periphery of bridging formamidinates.

The Ru_2 core may influence the C≡C–Ph ligand through three distinctive bonding modes illustrated in Scheme 3 with a generic C≡Y ligand (Y = CR, N, and O): the Ru–C σ bond (I), the $\pi^*(Ru{-}Ru) \rightarrow \pi^*(C{\equiv}Y)$ backdonation (II), and the $\pi(C{\equiv}Y){-}\pi^*(Ru{-}Ru)$ interaction (III). Although the filled/filled π–π interaction (III) is insignificant in complexes containing strong π-acid ligands such as CO, such interaction is the dominant metal–acetylide π-interaction in both $CpFeL_2(C{\equiv}CR)$ [25–27] and $ML_2(C{\equiv}CR)_2$ (L = neutral ligand, M = Pd, Pt) [28]. The strength of the filled/filled π–π interaction may be amplified in $Ru_2(form)_4(C{\equiv}CPh)$ compounds due to both the half-occupancy of π*(Ru) and the higher formal charge of the Ru center (3+).

An increase in the electron-withdrawing ability (the Hammett constant σ) of the aryl substituent decreases the electron density at the Ru_2 core, which reduces the π-donating ability and concurrently enhances both the σ- and π-accepting ability of the Ru center. If the $\pi^*(Ru{-}Ru) \rightarrow \pi^*(C{\equiv}C)$ backdonation (II) were dominant, a reduction in the Ru π-donating ability with an increase in σ would result in an increase in the strength of π(C≡C) bond, and the ρ value (the slope) of the Hammett plot (ν vs. ρ) would be positive. With the enhanced Ru σ- and π-acceptor abilities with increasing σ, on the other hand, the strength of the C≡C triple bond decreases as a result of the weakening of both the σ(C≡C) and π(C≡C) bonds. The value of ν(C≡C) should decrease with an increase in σ when either bonding modes I or II, or both are dominant. The negative ρ value obtained in the current Ru_2 series clearly indicates that the Ru_2 core affects the acetylide triple bond through both the $Ru{-}C_\alpha$ σ-bonding (I) and filled/filled $\pi^*(Ru{-}Ru){-}\pi(C{\equiv}C)$ interaction (III) instead of $\pi^*(Ru{-}Ru) \rightarrow \pi^*(C{\equiv}C)$ backdonation. Specific determination of the contributions from bonding modes I and III is possible with the aid of photoelectron spectra measurement [26,27] and higher level theoretical calculations, but cannot be achieved on the basis of the IR data gathered in the current study.

In previous studies of substituent-influences upon the M–C≡Y interaction for mononuclear complexes containing CO [29–32] and CN^- [33], positive values of ρ were obtained and a significant $d\pi(M) \rightarrow \pi^*(C{\equiv}Y)$ (Y as either O or N atom) backdonation was inferred. A similar conclusion was drawn for dirhodium carboxylates with axial CO ligands [34]. The contrast between the previous studies and our current results reflects the weak π-acceptor nature of the alkynyl ligand, which can only be 'induced' with electron-rich metal centers, as in the cases reported by Hopkins [23] and Bianchini [24].

3. Experimental

3.1. Starting materials and instruments

Diarylformamidines and $Ru_2(form)_4Cl$, the parent compound, were prepared as previously described [15,20]. Phenylacetylene and butyllithium (1.6 M in hexane) were purchased from Aldrich. THF was distilled over Na/benzophenone under a N_2 atmosphere prior to use. Silica gel (SIP® Brand 60 Å, 230–400 mesh) for flash column chromatography was obtained from Baxter. Infrared spectra were recorded on a Nicolet Magna 550 FT-IR spectrometer using KBr disks. UV-Vis spectral data (in CH_2Cl_2) were obtained with an IBM 9420 UV-Vis spectrophotometer. Magnetic susceptibilities were measured at 293 K with a Johnson Matthey magnetic susceptibility balance. Elemental analysis was performed by Atlantic Microlab, Norcross, Georgia. Cyclic voltammograms were recorded in 0.1 M $(n\text{-}Bu)_4NBF_4$ solution (CH_2Cl_2, N_2-degassed) on a BAS CV-50W voltammetric analyzer with the Pt working and auxiliary electrodes and a Ag | AgCl reference electrode. The concentration of diruthenium species was always 1.0 mM. The ferrocenium–ferrocene couple (internal reference) was measured at 625 mV under the experimental conditions.

3.2. Synthesis of $Ru_2(form)_4(C{\equiv}CPh)$

The parent compound $Ru_2(form)_4Cl$ (0.20 mmol) was suspended in distilled THF (30 ml) under argon. To this solution at 0°C was added PhC≡CLi (10 mmol, freshly prepared by treating PhCCH with equimolar Li-*n*-Bu in dry THF at −78°C under argon), whereupon the color immediately changed from dark green to dark red. After being stirred for 20 min, the reaction mixture was allowed to warm to room temperature. Stirring was continued until the color of the solution turned to a brownish yellow, and only at this point was the solvent removed under vacuum. After exposure to air, the purple residue was dissolved in 10 ml of CH_2Cl_2 and then loaded onto a short silica plug and eluted with CH_2Cl_2. The purple fraction was collected and evaporated to dryness by bubbling air through the solution at ambient temperature. The crude product was further purified on a silica gel column with CH_2Cl_2/hexane as the eluent (the exact ratio for each compound is given below). Volume reduction of the purple elute followed by alcohol precipitation (methanol or ethanol) yielded the crystalline product. Similar to the bis-adducts, the mono-adducts slowly decompose when heating above 50°C, even under the argon atmosphere.

3.2.1. $Ru_2(p\text{-}Clform)_4(CCPh)$ (**2**)

Eluent, CH_2Cl_2/hexane (v/v: 20/80). Yield, 40%. UV-vis, λ_{max} (nm, ε ($M^{-1}cm^{-1}$)): 597 (sh), 533 (8610), 381 (sh). IR (cm^{-1}, KBr disk): 2045(w), 1538(s), 1486(s), 1329(m), 1221(s), 1092(m), 1015(m), 959(w), 931(w), 826(m), 758(w), 698(w). Magnetic data: χ_{mol} (molar susceptibility), 4.81×10^{-3} emu; μ_{eff}, 3.61 BM. Anal. Calc. (found) for **2**·MeOH ($C_{61}H_{45}Cl_8N_8ORu_2$): C, 52.64 (52.98); H, 3.26 (3.26); N, 8.05 (8.09).

3.2.2. $Ru_2(m\text{-}Clform)_4(CCPh)$ (**3**)

Eluent, CH_2Cl_2/hexane (v/v: 60/40). Yield, 63%. UV-vis, λ_{max} (nm, ε (M^{-1} cm^{-1})): 590 (sh), 526 (8530), 379 (sh). IR (cm^{-1}, KBr disk): 2042(w), 1592(s), 1566(m), 1534(s), 1475(s), 1329(s), 1274(w), 1219(s), 1168(w), 1094(m), 1080(m), 1003(w), 970(m), 894(m), 784(m), 744(m), 692(s), 528(w), 437(m). Magnetic data: χ_{mol}, 5.82×10^{-3} emu; μ_{eff}, 3.92 BM. Anal. Calc. (found) for **3**·EtOH ($C_{62}H_{47}Cl_8N_8ORu_2$): C, 52.97 (52.92); H, 3.37 (3.31); N, 7.97 (7.96).

3.2.3. $Ru_2(m\text{-}CF_3form)_4(CCPh)$ (**4**)

Eluent, CH_2Cl_2/hexane (v/v: 25/75). Yield, 57%. UV-vis, λ_{max} (nm, ε (M^{-1} cm^{-1})): 585 (sh), 520 (9345), 373 (sh). IR (cm^{-1}, KBr disk): 2041(w), 1542(s), 1486(s), 1442(s), 1329(s), 1281(m), 1217(s), 1168(s), 1128(s), 1096(s), 1072(s), 999(w), 975(m), 895(m), 798(m), 762(m), 702(s), 665(m), 444(w). Magnetic data (293 K): χ_{mol}, 4.85×10^{-3} emu; μ_{eff}, 3.60 BM. Anal. Calc. (found) for **4** ($C_{68}H_{41}F_{24}N_8Ru_2$): C, 50.16 (50.35); H, 2.54 (2.57); N, 6.88 (6.84).

3.2.4. $Ru_2(3,4\text{-}Cl_2form)_4(CCPh)$ (**5**)

Eluent, CH_2Cl_2/hexane (v/v: 70/30). Yield, 43%. UV-vis, λ_{max} (nm, ε (M^{-1} cm^{-1})): 588 (sh), 536 (8945), 379 (sh). IR (cm^{-1}, KBr disk): 2034(m), 1588(w), 1541(s), 1464(s), 1329(m), 1259(w), 1215(m), 1131(m), 1033(m), 978(w), 906(w), 872(w), 821(w), 777(w), 755(w), 696(w), 543(w), 451(w). Magnetic data (293 K): χ_{mol}, 5.27×10^{-3} emu; μ_{eff}, 3.92 BM. Anal. Calc. (found) for **5** ($C_{60}H_{33}Cl_{16}N_8Ru_2$): C, 44.07 (44.47); H, 2.03 (2.13); N, 6.85 (6.86).

3.2.5. $Ru_2(3,5\text{-}Cl_2form)_4(CCPh)$ (**6**)

Eluent, CH_2Cl_2/hexane (v/v: 40/60). Yield, 54%. UV-vis, λ_{max} (nm, ε (M^{-1} cm^{-1})): 598 (sh), 527 (8790), 379 (sh). IR (cm^{-1}, KBr disk): 2031(m), 1584(m), 1562(s), 1533(s), 1427(m), 1332(m), 1252(w), 1219(m), 1113(m), 1003(m), 933(m), 853(w), 805(m), 754(w), 728(w), 699(w), 677(w). Magnetic data (293 K): χ_m, 5.94×10^{-3} emu; μ_{eff}, 3.99 BM. Anal. Calc. (found) for **6**·hexane ($C_{66}H_{47}Cl_{16}N_8Ru_2$): C, 46.05 (46.04); H, 2.75 (2.76); N, 6.51 (6.50).

3.3. X-ray data collection, processing, and structure analysis and refinement

Data collections were carried out with a Siemens R3m/V automated diffractometer using ω-scan on crys-

Table 3
Crystal and data collection parameters for compounds **3** and **6**

	3 · hexane	**6** · $4CH_2Cl_2$
Formula	$C_{66}H_{55}Cl_8N_8Ru_2$	$C_{64}H_{41}Cl_{24}N_8Ru_2$
Formula weight	1445.92	1975.0
Temperature (K)	294(2)	294(2)
Wavelength (Å)	0.71073	0.71073
Cryst syst	Monoclinic	Orthorhombic
Space group	$P2/n$ (# 13)	$Pbcn$(# 60)
a (Å)	11.616(3)	16.286(5)
b (Å)	15.970(4)	30.222(8)
c (Å)	16.573(4)	16.217(5)
α (°)	90	90
β (°)	105.88(2)	90
γ (°)	90	90
Volume (Å^3)	2957(1)	7982(4)
Z	2	4
Density (calculated) (g cm^{-3})	1.624	1.643
Absorption coefficient (mm^{-1})	0.923	1.226
F(000)	1462	3908
Crystal size (mm)	$0.50\times0.25\times0.10$	$0.60\times0.50\times0.50$
θ range for data collection (°)	1.81 to 27.50	1.84 to 22.53
Index ranges	$0\le15$, $0\le20$, $-21\le20$	$-17\le17$, $-32\le32$, $0\le27$
Reflections collected	7123	14173
Independent reflections	6797 ($R_{int}=0.0815$)	5240 ($R_{int}=0.1079$)
Refinement method	Full-matrix least-squares on F^2	Full-matrix least-squares on F^2
Data/restraints/parameters	6796/32/376	5240/159/501
Final R indices ($I>2\sigma(I)$)	R_1 [a,b] = 0.0928	R_1 [a] = 0.0524, wR_2 [b] = 0.1163
R indices (all data)	R_1 [a] = 0.0898, wR_2 [b] = 0.0977	R_1 [a] = 0.0976, wR_2 [b] = 0.1223
Goodness-of-fit on F^2 [c]	0.652	0.744
Extinction coefficient	0.00082(14)	0.00032(9)
Largest diff. Peak/hole (e Å^{-3})	0.772 and −0.570	0.408 and −0.440

[a] $R1=\Sigma\|\|F_o\|-\|F_c\|\|/\Sigma|F_o|$.
[b] $wR2=[\Sigma[w(F_o^2-F_c^2)^2]/\Sigma[w(F_o^2)^2]]^{1/2}$.
[c] Goodness-of-fit $=[\Sigma[w(F_o^2-F_c^2)^2]/(n-p)]^{1/2}$.

tals wedged into 0.5 mm glass capillaries filled with mother liquor-mineral oil mixture. A total of 6797 independent reflections were collected for **3** ($\theta\le27.5°$) and 5240 for **6** ($\theta\le22.53$). An empirical absorption correction was applied for **3** near the end of refinement but none for **6**.

All of the non-hydrogen atoms on the diruthenium complexes were located with direct methods and refined with anisotropic vibrational terms. The final model for **6** included two dichloromethane molecules per complex, and each solvent molecule is disordered over two conformations. One half of the hexane molecule is modeled near the crystallographic 2-fold axis in **3**. Positions of hydrogen atoms were calculated and assigned the isotropic thermoparameters $U(H)=1.2U_{eq}(C)$. Crystallographic computations were performed with both SHELXS-86 [35] and SHELXL-93 [36]. Relevant information on the data collection and the figure of merit of final refinement are listed in Table 3.

Acknowledgements

We thank the support from the Petroleum Research Fund/ACS and Florida Solar Energy Center (TR), and the Office of Naval Research (EJV and JDZ), and Professor M.D. Hopkins for providing the preprint of Ref. [23]. Insightful comments about the filled/filled π–π interaction from a reviewer are greatly appreciated.

References

[1] C. Lin, T. Ren, E.J. Valente, J.D. Zubkowski, J. Chem. Soc. Dalton Trans. (1998) 571.
[2] J. Manna, K.D. John, M.D. Hopkins, Adv. Organomet. Chem. 38 (1995) 79, and the earlier references therein.
[3] P.J. Stang, F. Diederich (Eds.), Modern Acetylene Chemistry, Weinheim, VCH, 1995.
[4] N. Hagihara, K. Sonogashira, S. Takahashi, Adv. Polym. Sci. 40 (1980) 149.
[5] J. Lewis, M.S. Khan, A.K. Kakkar, B.F.G. Johnson, T.B. Marder, H.B. Fyfe, F. Wittman, R.H. Friend, A.E. Dray, J. Organomet. Chem. 425 (1992) 165.
[6] M.G. Humphrey, Chem. Aust. 63 (1996) 442.
[7] (a) P.J. Stang, B. Olenyuk, Acc. Chem. Res. 30 (1997) 502. (b) P.J. Stang, Chem. Eur. J. 4 (1998) 19.
[8] M.H. Chisholm, Angew. Chem. Int. Ed. Engl. 30 (1991) 673.
[9] A.R. Chakravarty, F.A. Cotton, Inorg. Chim. Acta 113 (1986) 19.
[10] C.-L. Yao, K.H. Park, A.R. Khokhar, M.-J. Jun, J.L. Bear, Inorg. Chem. 29 (1990) 4033.
[11] J.L. Bear, B. Han, S. Huang, J. Am. Chem. Soc. 115 (1993) 1175.
[12] J.L. Bear, B. Han, S. Huang, K.M. Kadish, Inorg. Chem. 35 (1996) 3012.
[13] J.L. Bear, Y. Li, B. Han, E.V. Caemelbecke, K.M. Kadish, Inorg. Chem. 36 (1997) 5449.
[14] (a) T.C. Stoner, W.P. Schaefer, R.E. Marsh, M.D. Hopkins, J. Cluster Sci. 5 (1994) 107. (b) T.C. Stoner, R.F. Dallinger, M.D. Hopkins, J. Am. Chem. Soc. 112 (1990) 5651. (c) T.C. Stoner, S.J. Geib, M.D. Hopkins, J. Am. Chem. Soc. 114 (1992) 4201. (d) T.C. Stoner, S.J. Geib, M.D. Hopkins, Angew. Chem. Int. Ed. Engl. 32 (1993) 409. (e) K.D. John, S.J. Geib, M.D. Hopkins, Organometallics 15 (1996) 4357.
[15] C. Lin, T. Ren, E.J. Valente, J.D. Zubkowski, E.T. Smith, Chem. Lett. (1997) 753.
[16] F.A. Cotton, R.A. Walton, Multiple Bonds between Metal Atoms, Oxford University Press, Oxford, 1993.
[17] I.R. Whittall, M.G. Humphrey, D.C.R. Hockless, Aust. J. Chem. 50 (1997) 991.
[18] I.R. Whittall, M.G. Humphrey, D.C.R. Hockless, Aust. J. Chem. 51 (1998) 219.

[19] C. Lin, J.D. Protasiewicz, E.T. Smith, T. Ren, J. Chem. Soc. Chem. Commun. (1995) 2257.
[20] C. Lin, J.D. Protasiewicz, E.T. Smith, T. Ren, Inorg. Chem. 35 (1996) 6422.
[21] C. Lin, J.D. Protasiewicz, T. Ren, Inorg. Chem. 35 (1996) 7455.
[22] P. Zuman, The Elucidation of Organic Electrode Processes, Academic Press, NY, 1969.
[23] K.D. John, T.C. Stoner, M.D. Hopkins, Organometallics 15 (1997) 4948.
[24] C. Bianchini, A. Meli, M. Peruzzini, A. Vacca, F. Laschi, P. Zanello, F.M. Ottaviani, Organometallics 9 (1990) 360.
[25] N.M. Kostic, R.F. Fenske, Organometallics 1 (1982) 974.
[26] D.L. Lichtenberger, S.K. Renshaw, R.M. Bullock, J. Am. Chem. Soc. 115 (1993) 3276.
[27] D.L. Lichtenberger, S.K. Renshaw, A. Wong, C.D. Tagge, Organometallics 12 (1993) 3522.
[28] J.N. Louwen, R. Hengelmolen, D.M. Grove, A. Oskam, R.L. DeKock, Organometallics 3 (1984) 908.
[29] T.E. Bitterwolf, Polyhedron 7 (1988) 1377.
[30] P.B. Graham, M.D. Rausch, Organometallics 10 (1991) 3049.
[31] M.S. Blais, M.D. Rausch, Organometallics 13 (1994) 3557.
[32] P.G. Gassman, P.A. Deck, Organometallics 13 (1994) 1934.
[33] C. Nataro, J. Chen, R.J. Angelici, Inorg. Chem. 37 (1998) 1868.
[34] M.C. Pirrung, A.T. Morehead, J. Am. Chem. Soc. 116 (1994) 8991.
[35] G.M. Sheldrick, Program for crystal structure determination, University of Göttingen, Germany, 1990.
[36] G.M. Sheldrick, Program for refinement of crystal structure, University of Göttingen, Germany, 1993.